Am J Cancer Res 2016;6(5):1026-1039
www.ajcr.us /ISSN:2156-6976/ajcr0025581

Original Article

Anti-ABCG2 scFv antibody of lung adenocarcinoma increases chemosensitivity and induces apoptosis through the activation of mitochondrial pathway

Wen-Si Zhao[1,2*], Yi Luo[1*], Bo-Yi Li[1,2], Han-Jing Zhou[1,2], Tao Zhang[1]

[1]*Department of Oncology, The First Affiliated Hospital of Chongqing Medical University, Chongqing, China;* [2]*Chongqing Key Laboratory of Molecular Oncology and Epigenetics, The First Affiliated Hospital of Chongqing Medical University, Chongqing, China.* [*]*Equal contributors.*

Received February 4, 2016; Accepted February 12, 2016; Epub May 1, 2016; Published May 15, 2016

Abstract: ABCG2 is a multidrug resistance efflux pump expressed in many diverse tumors. The overexpression of ABCG2 is associated with resistance to a wide variety of anticancer agents, providing a noticeable setback to successful cancer therapy. Therapies targeting ABCG2 may therefore be a promising candidate for reversal of chemoresistance. The anti-ABCG2 single-chain variable fragment (scFv) antibody was constructed by phage display peptide library technology. Immunoblotting, ELISA and immunocytochemistry were used to evaluate the soluble expression and immunoreactivity of the scFv. The effects of scFv on cell function and chemosensitization were confirmed by colony formation, cell migration and CCK-8 assays. Flow cytometry was used to analyse the cell cycle and apoptosis. Radioimmunoimaging and nude mouse tumorigenicity assays were taken to determine the biodistribution and antitumor capacity of the scFv antibody. We have successfully screened out the candidate scFv antibody with an apparent molecular weight of 34 kDa. The scFv demonstrated favourable binding ability to lung adenocarcinoma cells and ABCG2 antigen, and the radioactivity was specifically aggregated at the tumor location. Furthermore, the internalized scFv resulted in antibody-mediated downregulation of ABCG2, proliferation inhibition, apoptosis and cisplatin (DDP) sensitivity. The anti-ABCG2 scFv antibody possesses good tumoraffin and antitumor activity and may therefore be an effective therapeutic agent for lung adenocarcinoma that is dependent on ABCG2 for drug resistance and survival.

Keywords: Lung adenocarcinoma, ABCG2, scFv, chemosensitization, radioimmunoimaging

Introduction

Lung cancer is the most commonly diagnosed cancer globally and tops the list for cancer-related mortality in both genders [1]. Lung adenocarcinoma has now become the most predominant subtype, representing over 38.5% of all lung cancer cases. Despite the development of new diagnostic technologies, surgical techniques and biologic therapies, the overall 5-year survival rate remains at a stagnant ~15% [2]. Refractoriness to chemotherapy remains the main aspect of the metastasis and relapse of primary tumor [3]. At present, none of available resistance-modulating strategies have been proven to be clinically useful in lung adenocarcinoma [4].

ATP-binding cassette (ABC) transporters play a crucial role in maintaining multidrug resistance (MDR), and high expression of these proteins is associated with tumor metastasis, recurrence and resistance to conventional chemoradiotherapy [5]. ABCG2, also known as breast cancer resistance protein (BCRP), is a new member of the ABC family, and has also been regarded as a potential biomarker of tumor-initiating cells (TICs) [6]. Studies have suggested that the overexpression of ABCG2 is responsible for therapy failure and poor clinical outcome [7-10]. Thus, ABCG2 may serve as an attractive candidate molecular target to reverse drug resistance and maximize the curative potential in cancer intervention.

In recent years, the scFv antibody has gained popularity in targeted therapy due to the smaller size, fast penetration, tight binding to target tissue, fast clearance from the body, and better pharmacokinetic properties as well as its fully

human origin [11, 12]. Phage display technology is still one of the most commonly used formats for generating recombinant antibody, as a result of the robustness coupled with the flexibility [13-15].

In this report, we attempted to construct a phage displayed scFv antibody against ABCG2 of lung adenocarcinoma. Subsequently, we radiolabeled the scFv antibody and investigated its tumor uptake and biodistribution in mice bearing ABCG2$^+$A549 tumor xenografts to evaluate the tumor targeting capability. Finally, we explored the underlying mechanisms of the proliferation inhibition and chemosensitization of this scFv. Our findings shed light on the anticancer activity of scFv antibody against ABCG2 and may provide a novel promising approach for molecular targeting therapy of lung adenocarcinoma.

Materials and methods

Reagents and cell culture

The filamentousphage display system was purchased from Pharmacia, Co. (Stockholm, Sweden). ABCG2 recombinant protein was purchased from Abnova Co. (Taibei, Taiwan). Mouse monoclonal antibody against ABCG2 and M13-HRP and rabbit polyclonal antibody against E-tag were purchased from Abcam Inc. (Cambridge, MA, USA). Rabbit monoclonal antibody directed against MDR1, Bcl-2, Bcl-xL, Bax, β-actin and HRP-conjugated anti-rabbit and anti-mouse IgG secondary antibodies were purchased from Cell Signalling Technology, Inc. (Danvers, MA, USA). FITC-conjugated anti-mouse IgG antibody was purchased from Earth Ox, LLC. (San Francisco, CA, USA). DDP was obtained from Sigma-Aldrich Co. (St. Louis, MO, USA). All other chemicals and solvents were of the highest analytical grade available.

The human lung adenocarcinoma cell lines A549 and H1975, the nasopharyngeal cancer cell line CNE2 and the colon cancer cell line HCT116 were obtained from American Type Culture Collection (ATCC, Rockville, MD). All cell lines were cultured in RPMI-1640 (Gibco, Karlsruhe, Germany) supplemented with 10% foetal bovine serum (FBS; Gibco) and 1% penicillin/streptomycin under a humidified atmosphere of 5% CO_2 at 37°C. Cells in the logarithmic phase of growth were used for all experiments.

Production and biopanning of the scFv antibody

A phage displayed library of scFv was developed as described previously [16]. Metastatic lymph nodes of 10 lung adenocarcinoma patients were collected for total RNA extraction using TRIzol (Invitrogen, USA). IgG-specific variable heavy (VH) and light (VL) chain gene fragments were amplified by PCR and then used as templates to extend a linker. ScFv gene was synthesized by SOE-PCR, then linked to a pCANTAB5E phagemid vector and transformed into electrocompetent E. coli TG1. The bacterium solutions were scattered on SOBAG agar plates. Plasmid PCR and Sfi I and Not I (New England Biolabs, UK) double digestion reactions were performed to identify the positive insert clones.

The primary library was phage-rescued using the M13KO7 helper phage and the specific scFv antibody was isolated by the biopanning process according to the manual. After three rounds of panning against A549 cells, three other rounds were performed against ABCG2 antigen. The eluted phages were serially diluted to infect the log phase E. coli TG1 to estimate the titers. Phage ELISA was performed to investigate the affinity for ABCG2 purified antigen of the desired scFv. Clones with high affinity were selected for further evaluation.

Soluble expression of the scFv antibody

Strongly positive clone was selected to infect log-phage E. coli HB2151. Expression of soluble scFv was induced by adding isopropyl β-D-thiogalactopyranoside (IPTG) to a final concentration of 1 mmol/L. Ice-cold TES (10 mM Tris-HCl, 1 mM EDTA, 1 mM SDS) solution was added to induce a mild osmotic shock, and the mixture was then centrifuged at 12 000 r/min for 10 min. The supernatant containing the soluble antibodies from the periplasm, was purified and transferred to clean tubes and stored at -20°C. The concentration of scFv was determined. The proteins were separated on 12% gels and visualized by Coomassie Brilliant Blue staining. For Western blotting, the separated proteins were transferred on to a polyvinylidene difluoride (PVDF) membrane (Bio-Rad, CA,

USA), incubated with a primary antibody against E-tag. Antibody binding was visualized by enhanced chemiluminescence (Bio-Rad).

ELISA and immunocytochemistry

Specificity of scFv antibody toward lung adenocarcinoma cells was evaluated by ELISA and ICC. For ELISA, A549 cells, H1975 cells, CNE2 cells and HCT116 cells were seeded into 96-well ELISA plates (1×10^4 cells/well) and cultured overnight. There was no significant difference in the ABCG2 expression level of these cell lines (additional file 1: Table S1; file 2: Figure S1 and S2). After being blocked with 1% BSA/PBS, cells were washed thrice with 0.1% TBST and 10 μg scFv per well were added to incubate overnight at 4°C, and non-targeting scFv antibody (primary scFv before biopanning) was used as a control. The rabbit anti-E tag antibody and HRP conjugated secondary antibody were successively added and incubated for 1 h at 37°C. The presence of HRP was detected with tetramethylbenzidine (TMB) as substrate. Absorbance at 490 nm was measured using a microplate reader. For competitive ELISA, we mixed the scFv (1 mg/ml) and IgG (1 mg/ml) in different ratios as well as IgG alone added into each well and performed the ELISA experiment as described above. Affinities were determined as the inhibition rates represented by ELISA readings. For immunocytochemistry (ICC), cells at the density of 1×10^4 cells/well were seeded into 96-well plates and incubated with scFv (10 μg/well) at 4°C overnight, washed with PBS and incubated with the HRP conjugated anti-E tag antibody. Binding was detected using diaminobenzidine (DAB) as the substrate.

Labeling the scFv antibody with radionuclide and SPECT/CT imaging

The scFv was labelled with ^{131}I using the chloramine T method. Briefly, 50 μl of scFv antibodies (1 mg/ml) were incubated with 35 μl of ^{131}I (11.0 mCi/ml) for 3 min. Subsequently, 100 μl of chloramine T (2 mg/ml) was added for a 40-s reaction followed by a 1 min reaction with 100 μl of sodiumpyrosulfite (2 mg/ml), 100 μl of 1% kalium iodidum (KI) was added to terminate the labelling process. The ^{131}I-labelled scFv was purified by gel-filtration on Sephadex G50 Column (GE Healthcare, USA) and the non-targeting scFv labelled with ^{131}I was used as a control. Tumor-bearing mice were used for the biodistribution study. ABCG2$^+$A549 cells (2×10^6) were implanted subcutaneously into the right shoulder area. When tumors reached 500 mm^3, mice were injected via the tail vein with 200 μl of purified ^{131}I-labelled scFv (approximately10 μCi/g). Three mice were sacrificed at 6, 12, 24, and 48 h after injection, respectively. The tumor, blood, muscle, brain and other major organs of interest were removed, weighed, and counted for radioactivity in a gamma counter. The results are expressed as the percent injected dose per gram of tissue (% ID/g). Immunoreactivity of ^{131}I-labelled antibody was analysed by dose-dependent cell binding assays. The mixture of scFv and free ^{131}I was used as a control.

For radioimmunoimaging analysis, the tumor-bearing mice were fed with water containing 1% KI for 3 days prior to imaging to block the thyroids and then injected with ^{131}I-labelled scFv as above described. The primary scFv antibody labelled with ^{131}I was used as a control. Mice were scanned at designated times (SPECT-CT Symbia T2, Siemens, Germany). CT images were acquired in 30 projections with a 1000 ms exposure time using a 45 kVP X-ray source over 5 min. Whole-body radionuclide images were reconstructed using the iterative ordered-subset expectation maximization (OSEM) algorithm, and fused with CT images.

Growth inhibition and cell viability assays

To directly link antibody effect with ABCG2, ABCG2$^+$ and ABCG2$^-$ lung adenocarcinoma cells were sorted by fluorescent activated cell sorting (FACS). Cells were then seeded into 96-well plates at 5×10^3 cells/well overnight and incubated with purified scFv (at near IC_{50} concentration: 10 μg/well) at 37°C. The effect of scFv on cell proliferation was measured according to the protocol of CCK-8 (Dojindo, Japan). All plates had control wells containing medium without cells to obtain a value for background spectrometric absorbance, which was subtracted from the test sample readings.

For colony formation assay, cells were seeded into six-well plates (1000 cells/well) with 2 ml medium. ScFv (0, 10 and 20 μg) were added next day, and the medium was changed every 3-4 days. After 14 days, cells fixed with methanol and stained with 0.1% crystal violet. Visible colonies (≥100 cells per colony) were manually counted and photographed. The cloning effi-

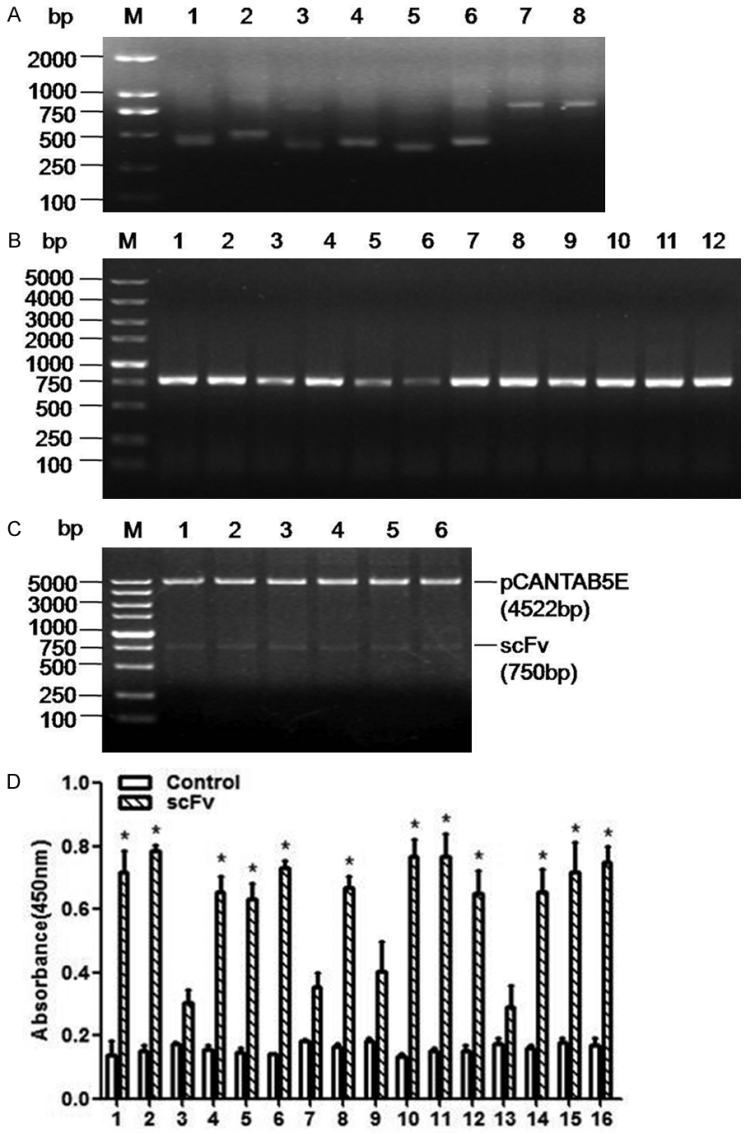

Figure 1. Library construction. A. PCR amplification of the VH, VL (Vκ/Vλ) and scFv fragments. Lane M: DL2000 DNA ladder; lane 1, 3, 5: VH (360 bp), Vκ/Vλ (340 bp); lane 2, 4, 6: VH-Linker- (410 bp), Linker+-Vκ/Vλ (390 bp); lane 7 to 8: scFv (750 bp). B. Plasmid PCR. Lane1 to 12: twelve colonies chose randomly, lane M: DL5000 DNA ladder. C. Dual-enzyme digestion. Lane1 to 6: Six positive plasmids, lane M: DL5000 DNA ladder. The scFv and pCANTAB 5E vector were approximately 750 bp and 4522 bp. D. Phage ELISA. 12 of 16 (75%) independent clones were positive for binding to ABCG2 antigen (*P/N > 4).

ciency (%) = (the number of clones/the number of seed cells) × 100%.

Cell migration assays were performed using 24-well Transwell plates (8 μm pore size; Corning). Cells (1.0×10^5 cells/well) in serum-free medium containing different concentrations of scFv (0, 10 and 20 μg) and migration-inducing medium (with 5% FBS) were added separately to the upper and lower chambers. After 24 h, the top surface of the chambers was scraped using a cotton swab, and the cells on the lower surface of the membranes were fixed with methanol, stained with Giemsa solution and counted using light microscopy.

For cytotoxicity assay, cells pretreated with different concentrations of scFv for 48 h were then seeded into a 96-well plate at a density of 5×10^3 cells/well, and cultured in medium containing increasing concentrations of DDP for 24 h. At the end of the drug exposure duration, cell viability was measured by CCK-8 assay. The half inhibitory concentration (IC_{50}) values were calculated to evaluate the degree of chemosensitization.

Apoptosis and cell cycle analyses

For apoptosis analysis, briefly, after 48 h of scFv treatment (0, 10 and 20 μg), cells were collected and washed with ice-cold PBS twice and subjected to annexinV-FITC/PI (KEYGEN Biotech, Nanjing, China) staining for 15 min in the dark at RT. The cell fluorescence was measured by the FACS Calibur (BD Biosciences, San Jose, CA). For cell cycle analysis, cells were harvested, and fixed with ice-cold 70% ethanol overnight at 4°C after treatment with scFv. Cells were then washed, resuspended and stained with PI/RNase staining buffer (BD Biosciences) at 37°C for 30 min. The cell cycle profiles were obtained by flow cytometry at 488 nm, and the data were analysed using Cell Quest Software (BD Biosciences).

Immunoblotting

Cell lysates of $ABCG2^+$ and $ABCG2^-$ lung adenocarcinoma cells incubated with different concentrations of scFv were prepared according to

Table 1. Biopanning scFv antibody library

Rounds of biopanning	Phage titer (cfu/ml)		Yield (%)
	Phage input	Phage output	
1	3.76×10^{12}	5.8×10^{6}	1.54×10^{-6}
2	2.5×10^{12}	6.2×10^{6}	2.48×10^{-6}
3	3.54×10^{11}	7.8×10^{6}	2.2×10^{-5}
4	2.8×10^{11}	8.85×10^{6}	3.16×10^{-5}
5	2.0×10^{11}	2.52×10^{7}	1.26×10^{-4}
6	1.8×10^{11}	3.06×10^{7}	1.7×10^{-4}

the method described by the protein extract kit (KEYGEN Biotech). Protein concentrations were determined using the BCA method. Cell lysates were analysed for western blots using ABCG2, MDR1, Bcl-2, Bcl-xL, Bax and β-actin. Antibody binding was visualized by enhanced chemiluminescence (Bio-Rad). Densitometric analysis was performed using Image Pro Plus software and normalized to β-actin.

In vivo experiments

BALB/c nude mice (4-6 weeks old) were provided by the Experimental Animal Centre of Chongqing Medical University, China. To generate xenograft models, freshly dissociated ABCG2^{+}A549 cells (2×10^{6}/100 μl PBS) were subcutaneously injected into the back of each mouse. Tumor growth and volumes were monitored every other day using a digital calliper according to the formula V=1/2 × length × width^{2}. When the average tumor size reached approximately 500 mm^{3}, mice were then divided randomly into four groups: (1) normal saline (NS); (2) scFv alone; (3) DDP alone; and (4) pretreatment with scFv followed by DDP, with four in each group, and subjected to the corresponding treatment. The therapy used in this study was scFv 10 mg/kg, i.p., d1-3 and DDP 2.5 mg/kg, i.p., d 4, 7. There were no treatment-related deaths until termination. All mice were sacrificed by cervical dislocation. Tumors were then removed, weighed, and prepared for immunohistochemistry (IHC) analysis. All the animal studies were approved by the Animal Ethics Committee of Chongqing Medical University.

Immunohistochemistry

Tumor tissues were fixed in 4% formaldehyde solution and subsequently embedded in paraffin. IHC studies were performed using the standard streptavidin-peroxidase method with the Ultra Sensitive SP link Detection Kit (ZSGB-Bio, Beijing, China) according to the manufacturer's instructions. Tumor specimens were stained using Ki-67 and cleaved caspase 3 antibody (Cell Signaling Technology, Danvers, MA) for cell proliferation and apoptosis. Immunostained slides were blindly evaluated by a trained pathologist under a transmission light microscope.

Statistical analysis

Data are graphically represented as the mean ± standard error of the mean (SEM). All of the experiments were performed at least in triplicate and representative results are presented. Student's t-test and two-way ANOVA were performed with GraphPad Prism 5.0 software (La Jolla, CA, USA). A p value of less than 0.05 was considered significant.

Results

Library construction and panning

The presence of VH, VL and scFv gene fragments was confirmed by electrophoresis, with their sizes were approximately 360 bp, 340 bp and 750 bp (**Figure 1A**). Plasmid PCR and double digestion reactions (**Figure 1B**, **1C**) revealed that the positive insert ratio was approximately 100% (12/12). Rescued by M13KO7 helper phage, the recombinant phage antibody library (approximately 10^{11} cfu/ml) was constructed. After six rounds of biopanning, individual phage-displayed scFv fragments were tested for reactivity with ABCG2 antigen by phage ELISA. Of the 16 screened clones, 12 were positive which means the positive recognition rate can reach 75% (**Figure 1D**). The biopanning process resulted in a 110-fold enrichment of affinity (**Table 1**).

Expression and purification of the soluble scFv antibody

The scFv was stably expressed in E. coli HB-2151 transfected with positive phage clone and purified from the culture supernatant using a HiTrap™ Anti-E Tag column (Pharmacia). The expressed and purified scFv was loaded on 12% SDS-PAGE and analysed by Western blot. This protein migrated with a molecular mass approximately 34 kDa (**Figure 2A**).

Immunoreactivity of the scFv antibody

The immunoreactivity of scFv was determined by ELISA and ICC. Results revealed that the scFv antibody has relatively specificity that could bind to A549 and H1975 cells compared

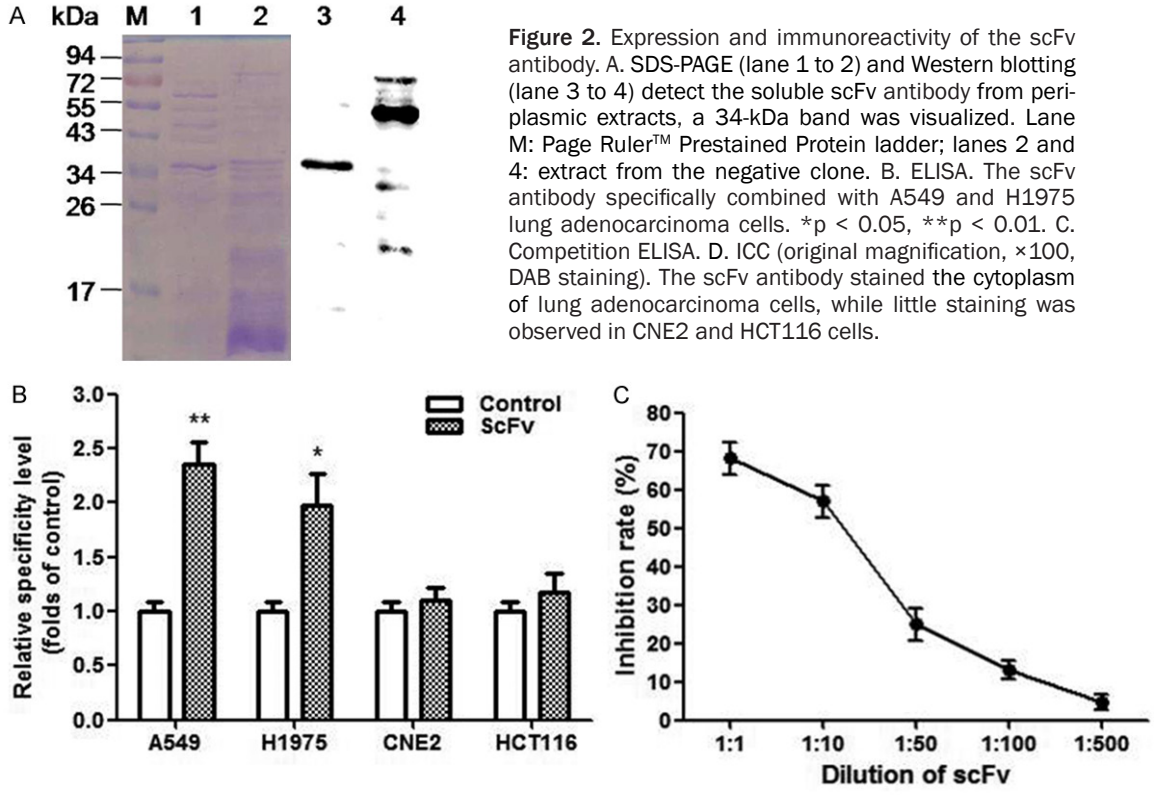

Figure 2. Expression and immunoreactivity of the scFv antibody. A. SDS-PAGE (lane 1 to 2) and Western blotting (lane 3 to 4) detect the soluble scFv antibody from periplasmic extracts, a 34-kDa band was visualized. Lane M: Page Ruler™ Prestained Protein ladder; lanes 2 and 4: extract from the negative clone. B. ELISA. The scFv antibody specifically combined with A549 and H1975 lung adenocarcinoma cells. *$p < 0.05$, **$p < 0.01$. C. Competition ELISA. D. ICC (original magnification, ×100, DAB staining). The scFv antibody stained the cytoplasm of lung adenocarcinoma cells, while little staining was observed in CNE2 and HCT116 cells.

with non-targeting scFv and other cancer cell lines (**Figure 2B**, **2D**). Competitive ELISA was performed to confirm antibody affinity. The scFv was tested at different concentrations (1:1, 1:10, 1:50, 1:100, 1:500 diluted). A high extracellular scFv concentration (1:1 diluted) showed a significant inhibitory effect in competition with the IgG antibody (inhibition rate, 68.09% ± 4.27%), while the inhibition rate of the low extracellular concentration group (1:500 diluted) descended to 4.56% ± 1.96% (**Figure 2C**).

Biodistribution of the scFv antibody and SPECT/CT imaging

The ^{131}I-labelled scFv antibody showed dose-dependent binding to lung adenocarcinoma cells in vitro (**Figure 3A**), and the distribution in vivo was also analysed. As shown in **Table 2**, the ^{131}I-labelled scFv exhibited rapid tumor uptake at a relatively high level, with an activity of 22.98% ± 2.85% ID/g at 6 h. Thereafter, the antibody retention in the tumor decreased over time. As expected, the activity of the ^{131}I-labelled scFv in blood and muscle was lower than that in tumor xenografts. The tumor-to-blood and tumor-to-muscle signal ratios at 6, 12, 24, and 48 h were 1.08 ± 0.10, 1.61 ± 0.44, 3.45 ± 1.06, 1.61 ± 0.30 and 3.09 ± 0.54, 3.17 ± 0.17, 4.51 ± 0.89, 3.37 ± 0.62. The peak ratio was reached at 24 h. Moreover, the lowest accumulation of the ^{131}I-labelled scFv was detected in the brain. The tumor-to-brain ratio increased from 12.08 ± 2.93 at 6 h to 23.65 ±

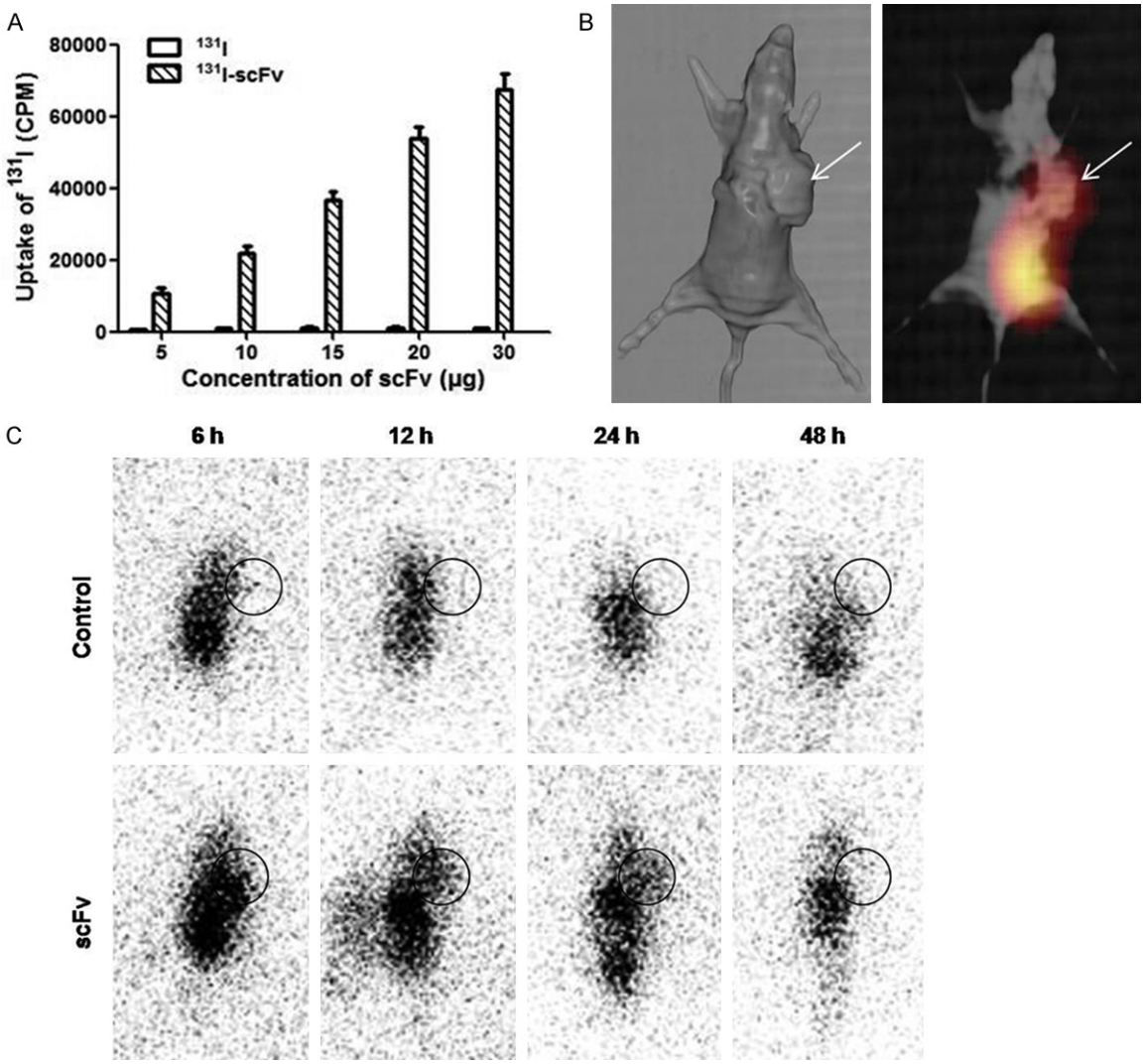

Figure 3. Radioimmunoimaging of the scFv antibody. A. Immunoreactivity of ^{131}I-scFv antibody was analysed using ABCG2^{+}A549 cell binding assays. The same amount of free ^{131}I was used as a control. B. The SPECT and CT images at 24 h were fused. The arrow indicates the tumor graft. C. After intravenous injection of the ^{131}I-labelled scFv and non-targeting scFv antibody, the tumor-bearing mice were scanned by SPECT at 6, 12, 24, and 48 h, respectively. The circle area is the ROI.

3.00 at 24 h, which was approximately 4-5 times higher than the tumor-to-muscle ratio at the same time point. Whole-body imaging by SPECT/CT further confirmed the tumor-specific internalization of the scFv antibody compared with non-targeting scFv (**Figure 3B**, **3C**). The region of interest (ROI) signal in tumors was 4.5 times greater than that in muscle, indicating that the antibody specifically accumulates in the tumor location.

ScFv antibody inhibits cell viability and increases DDP sensitivity

As shown in **Figure 4A** and additional file 3: Figure S3, we observed that scFv antibody dose- and time-dependently inhibited the proliferation of lung adenocarcinoma cells. Moreover, in both the colony formation and migration assays, scFv antibody significantly reduced the number of ABCG2^{+} cells that could establish a clone or migrate through the insert membrane compared with the ABCG2^{-} fraction (**Figure 4B**, **4C**).

To clarify whether the decreased cell viability was due to the induction of cell apoptosis, flow cytometry was further performed. Significantly increased apoptosis was found when cells were treated with 20 μg scFv antibody (47.95% ± 5.43% vs. 8.80% ± 2.51%, $P < 0.01$), which may partly contribute to the decreased cell prolifer-

Table 2. Tissue distribution of ^{131}I-labelled scFv antibody in tumor-bearing mice (n=3)

Tissue	6 h	12 h	24 h	48 h
Tumor	22.98 ± 2.85	10.74 ± 0.98	6.39 ± 0.54	1.41 ± 0.15
Blood	21.28 ± 1.63	7.37 ± 1.35	2.24 ± 0.64	0.90 ± 0.08
Heart	13.41 ± 1.38	6.02 ± 1.26	1.67 ± 0.19	0.61 ± 0.15
Liver	20.67 ± 2.18	11.03 ± 1.08	5.68 ± 0.34	1.35 ± 0.19
Spleen	18.81 ± 2.71	9.20 ± 1.90	4.25 ± 0.49	0.92 ± 0.19
Lung	17.41 ± 2.60	9.01 ± 1.39	3.35 ± 0.56	0.89 ± 0.04
Kidney	21.38 ± 1.59	14.02 ± 1.45	7.86 ± 0.42	1.77 ± 0.33
Brain	2.16 ± 0.60	0.74 ± 0.11	0.27 ± 0.02	0.07 ± 0.01
Intestine	18.58 ± 1.15	13.19 ± 1.04	6.20 ± 0.14	1.33 ± 0.29
Bone	12.22 ± 1.39	5.75 ± 1.00	2.15 ± 0.16	0.69 ± 0.15
Muscle	7.72 ± 1.05	3.40 ± 0.34	1.49 ± 0.20	0.43 ± 0.05
Ratio				
Tumor/brain	12.08 ± 2.93	14.92 ± 1.91	23.65 ± 3.00	21.65 ± 4.95
Tumor/muscle	3.09 ± 0.54	3.17 ± 0.17	4.51 ± 0.89	3.37 ± 0.62
Tumor/blood	1.08 ± 0.10	1.61 ± 0.44	3.45 ± 1.06	1.61 ± 0.30

Note: Tissue uptakes are expressed as percent injected dose per gram (% ID/g ± SEM).

ation and growth delay (**Figure 4D**). It is well known that there is a close relationship between cell cycle arrest and the inhibition of cell proliferation [17]. Subsequently, cell cycle analysis was performed. Compared with the control and ABCG2$^-$ group, an evident increase of G1 phase cells was observed in the 20 μg scFv-treated group (70.84% ± 1.93% vs.52.44% ± 2.72%, $P < 0.01$), accompanied by a decrease in the number of cells in S and G2 phases (**Figure 4E**).

Further, to investigate the effect of chemosensitization of the scFv antibody, ABCG2$^+$ and ABCG2$^-$ cells were treated with scFv antibody in combination with different concentrations of DDP. As shown in **Figure 4F**, combined treatment markedly decreased DDP concentration to achieve 50% growth inhibition when compared with DDP as a single treatment in the ABCG2$^+$ cells (5.73 ± 0.18 μg/ml vs. 1.09 ± 0.23 μg/ml, $P < 0.01$), and it also demonstrated a negative correlation between the IC_{50} value of DDP and scFv concentration. In ABCG2$^-$ cells, we did not observe this chemosensitization (5.60 ± 0.58 μg/ml vs. 5.12 ± 0.36 μg/ml, $P > 0.05$), which suggested that the scFv antibody might induce DDP sensitivity through the inhibition of ABCG2 activity.

ScFv antibody modulates ABCG2 expression and mitochondrial pathway

Since MDR1/P-gp was also extensively reported to be involved in multi-drug resistance [18, 19], the expression of ABCG2 and MDR1 was detected by Western blotting. As depicted in **Figure 5**, ABCG2 and MDR1 were found to be down-regulated by the scFv antibody in ABCG2$^+$ lung adenocarcinoma cells than their ABCG2$^-$ counterparts. To further confirm the induction of apoptosis of scFv antibody, the Bcl-2 family of proteins was detected. Data showed that the expression of Bcl-2 and Bcl-xL was visibly decreased, while the expression of Bax was steadily increased in a concentration-dependent manner. These results suggest that the mitochondrial pathway is involved in apoptosis of ABCG2$^+$ lung adenocarcinoma cells induced by the scFv antibody.

In vivo antitumor activity of the scFv antibody

A549 xenograft model was employed to validate the antitumor potential and increased DDP sensitivity of the scFv antibody in vivo. As shown in **Figure 6A**, smaller tumor volumes were observed in the combined group compared with that in single drug group and control group. Significantly decreased proliferation (Ki-67 staining) and increased apoptosis (cleaved caspase 3 staining) were detected in the tumor specimens of combined group (**Figure 6B** and additional file 4: Figure S4). These results are consistent with our findings in vitro, showing that the scFv antibody increased DDP sensitivity and significantly inhibited lung adenocarcinoma development.

Discussion

Drug resistance is a vast research field and the tolerance to chemotherapy is still the major cause of cancer lethality [20, 21]. Evidence is mounting that many cancers that express

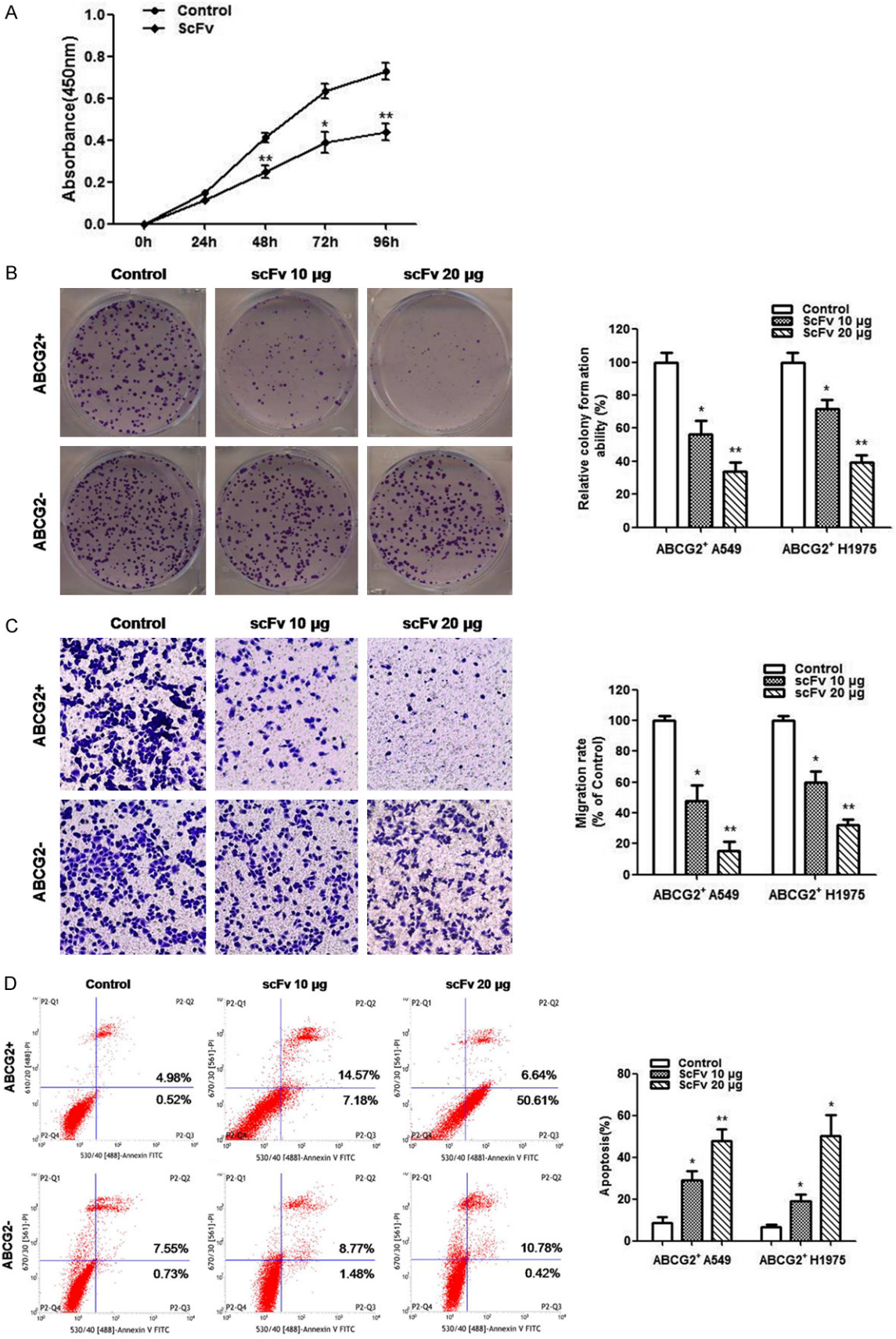
A
Control
ScFv
Absorbance(450nm)
1.0
0.8
0.6
0.4
0.2
0.0
0h
24h
48h
72h
96h
B
Control
scFv 10 μg
scFv 20 μg
ABCG2+
ABCG2-
Relative colony formation ability (%)
ABCG2+ A549
ABCG2+ H1975
C
Migration rate (% of Control)
D
4.98%
0.52%
14.57%
7.18%
6.64%
50.61%
7.55%
0.73%
8.77%
1.48%
10.78%
0.42%
Apoptosis(%)

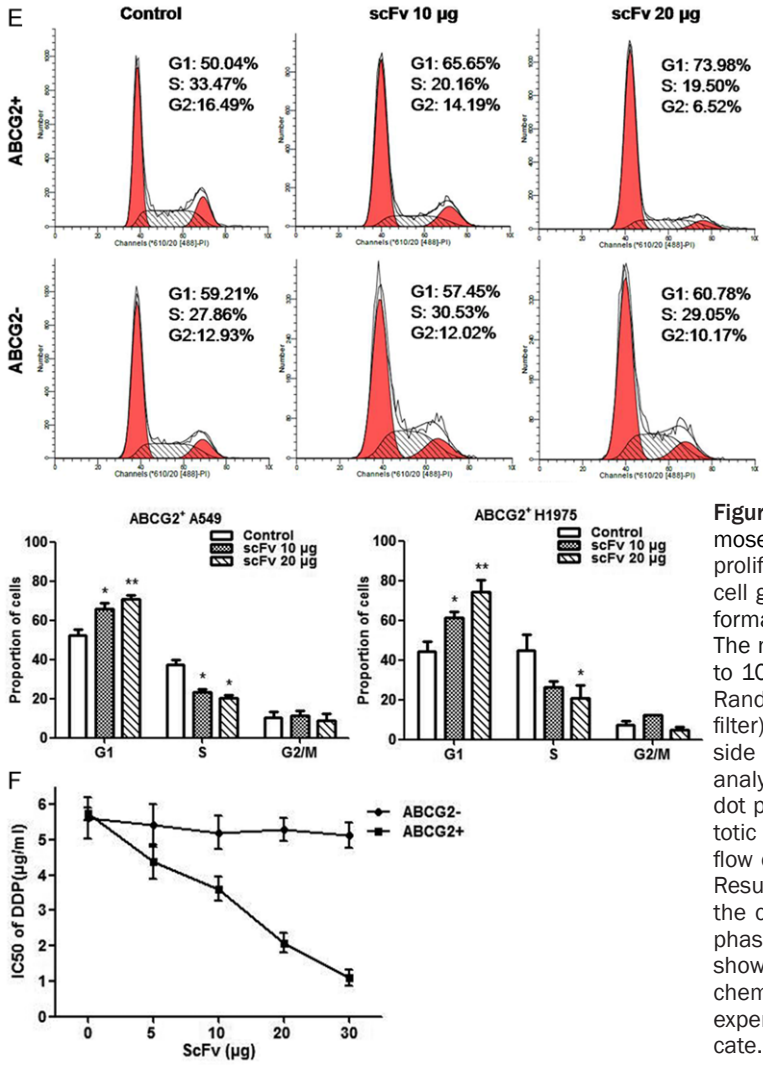

Figure 4. Proliferation inhibition and chemosensitization of the scFv antibody. A. Cell proliferation was evaluated by plotting the cell growth curve. B. Representative colony formation assay and quantitative analysis. The number of colonies in controls was set to 100%. C. The transwell migration assay. Random fields were scanned (four fields per filter) for the presence of cells on the lower side of the membrane. D. Cell apoptosis analysis by flow cytometry. Numbers inside dot plots indicate the percentages of apoptotic A549 cells. E. Cell cycle analysis by flow cytometry. DNA content was analysed. Results were presented as percentages of the cell population in G0-G1, S, and G2-M phases of the cell cycle. The upper panel shows the results of A549 cells. F. DDP chemosensitization of scFv antibody. All the experiments were performed thrice in triplicate. *$p < 0.05$, **$p < 0.01$.

ABCG2 exploit the property of the efflux pump to survive chemotherapy [22-24]. Two recent studies showed that when SCLC and advanced NSCLC patients received platinum-based combination chemotherapy, ABCG2 expression was significantly associated with a lower response rate to chemotherapy and shorter progression-free survival (PFS) and overall survival (OS) [8, 10].

Since lung cancer therapy focuses more on molecularly targeted therapy [25, 26]. Here, we managed to generate a bispecific scFv antibody of lung adenocarcinoma against ABCG2 through phage-displayed peptide library technology. We optimized the biopanning process with the combination of two panning strategies. First, screening directly on the surface of lung adenocarcinoma cells would maximize the diversity of the antibody library and conformational epitopes. Second, the solid phase panning on purified ABCG2 antigen might enhance the specificity of the antibody. Eventually, we produced a high-capacity phage antibody library and selected out desired scFv antibody with favourable specificity and affinity.

Receptor-mediated endocytosis and antibody-dependent cell cytotoxicity are crucial to the antitumor activity of antibody [27, 28]. ELISA and ICC indicated the specific binding capacity of the scFv antibody to lung adenocarcinoma cells, which laid the foundation for its subsequent functions. As expected, the scFv antibody as an immunoactive ligand together with its cytotoxic effects significantly inhibited cell proliferation, clonality and motility, and induced apoptosis and cell cycle arrest. It is likely that the scFv antibody utilized its cytotoxicity or activated cytosolic adhesion molecules and down-

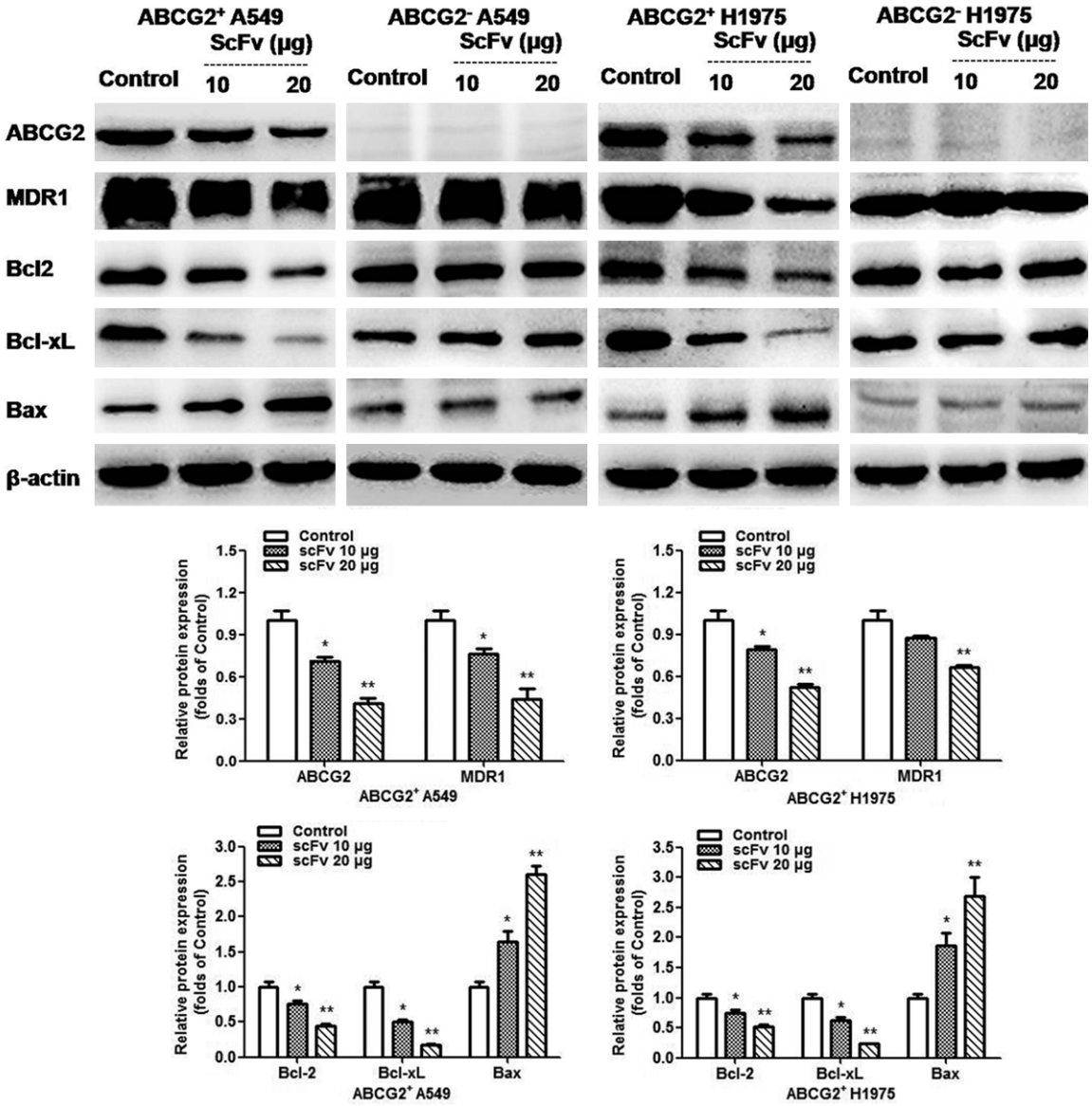

Figure 5. ScFv antibody regulates the ABCG2 expression and activates the Bcl-2 pathway. The expression of ABCG2, MDR1, Bcl-2, Bcl-xL and Bax was evaluated by immunoblotting. β-actin was used as an internal loading control. The blots shown were representative of six independent experiments. *$p < 0.05$, **$p < 0.01$.

stream signalling pathways to exert its efficacy in cancer immunotherapy. Among apoptotic regulatory proteins, the Bcl-2 family, which include both anti- and pro-apoptotic members, is key regulator [29]. The expression levels of Bcl-2, Bcl-xL and Bax further validated the potential mechanism of scFv antibody-induced apoptosis.

Our in vitro experiments with DDP treatment showed that the scFv antibody significantly increased the chemosensitivity to DDP. It was reported that DDP-induced cell apoptosis involved the activation of the Fas death receptor pathway independent of Fas ligand [30]. Since DDP is not known to be an ABCG2 substrate [31, 32], it is possible that the scFv antibody combining with ABCG2 epitope might activate the Fas receptor and facilitate DDP binding to the Fas-associated death domain protein (FADD) and thereby result in massive amplification of cytotoxicity and apoptosis. Downregulation of ABCG2 could potentially make Fas/DDP/FADD interactions more stable and durable. Additionally, the inhibition the process of recruitment of MDR1 to the active site by blocking the ABCG2 epitope may strengthen this chemosensitization.

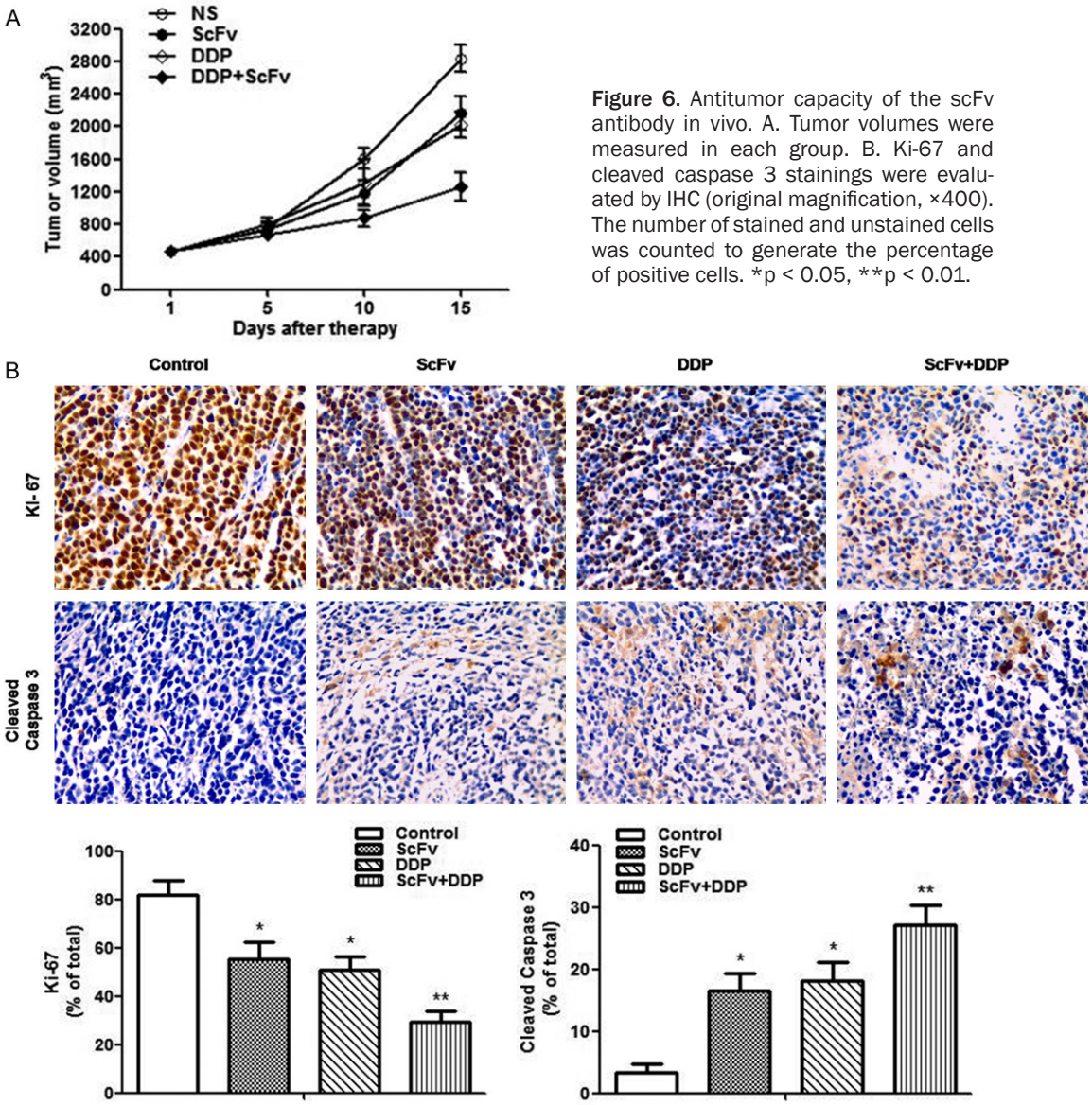

Figure 6. Antitumor capacity of the scFv antibody in vivo. A. Tumor volumes were measured in each group. B. Ki-67 and cleaved caspase 3 stainings were evaluated by IHC (original magnification, ×400). The number of stained and unstained cells was counted to generate the percentage of positive cells. *p < 0.05, **p < 0.01.

However, in vitro experiments may not perfectly reflect what is observed in primary cancer cells, whereas in vivo models are more conducive to the assessment of treatment responses. In xenograft models, we observed that the scFv treatment especially when combined with DDP resulted in remarkable suppression of tumor growth with smaller tumor volumes and increased numbers of apoptosis cells in the residual tumors. As is known that ABCG2 also plays an important role in the maintenance of the side population (SP) phenotype of cancer stem-like cells (CSCs), which are hypothesized to be the primary force driving tumor initiation, resistance to chemoradiotherapy and recurrence [33]. What is noteworthy is that if the ABCG2$^+$ subpopulation has CSC features, conventional observations of curative efficacy (tumor volume) might only suggest how the bulk tumor responds to treatment, failing to provide extra support for everlasting tumor eradicating potential. Seen in this light, other endpoints (such as tumor regrowth or relapse) should be added to evaluate therapeutic responses.

In mice bearing tumor xenografts, intravenously injected ^{131}I-labelled scFv antibody rapidly accumulated in tumors at a high level within 6 h. In addition, the activity of the ^{131}I-scFv antibody in the blood, kidney and liver decreased from 20% at 6 h to 1-2% at 48 h after injection, indicating the rapid kinetics of the antibody.

The relative satisfactory radioimmunoimaging effect and affinity to target tissues demonstrates its potential in lung adenocarcinoma immunotherapy as a delivery vehicle. However, the disassociation and degradation of ^{131}I from antibody would increase the active signal in the blood and result in a low ratio of tumor to blood. Therefore, other radioactive materials should be explored in future research. Simultaneously, scFv was localized to the spleen at a slightly high level that might produce antibody-dependent cell cytotoxicity. However, the potential interaction between this scFv antibody and splenocytes might also set the stage for transient toxicity of spleen and safety concerns. To decrease unintended side effects, several factors and parameters for biopanning could be optimized to lower retention times in non-target tissue and accelerate clearance from the body. In addition, developing higher affinity mutants of scFv through site-directed mutagenesis could also be considered in the future.

Taken together, a phage-displayed scFv antibody of lung adenocarcinoma against ABCG2 antigen was successfully prepared. The fully humanized scFv antibody exerted favourable effects in rapidly and specifically binding to lung adenocarcinoma cells and enhanced DDP cytotoxicity by targeting ABCG2. Our findings strongly suggest that the scFv antibody might be applied as a meaningful supplement for lung adenocarcinoma chemoresistance reversal and antibody targeted therapy.

Acknowledgements

We thank the Department of Cardiothoracic Surgery and Nuclear Medicine of the First Affiliated Hospital of Chongqing Medical University for helping us with clinical specimen acquisition and radioimmunoimaging studies. Supported by the National Natural Science Foundation of China: No. 81302018.

Declaration of conflict of interest

None.

Address correspondence to: Tao Zhang, Department of Oncology, The First Affiliated Hospital of Chongqing Medical University, No. 1 Youyi Road, Yuzhong District, Chongqing 400016, China. Tel: 86-2389012151; Fax: 86-68986810; E-mail: tumorzzt@163.com

References

[1] Siegel RL, Miller KD and Jemal A. Cancer statistics, 2015. CA Cancer J Clin 2015; 65: 5-29.

[2] Dela Cruz CS, Tanoue LT and Matthay RA. Lung cancer: epidemiology, etiology, and prevention. Clin Chest Med 2011; 32: 605-644.

[3] Dean M, Fojo T and Bates S. Tumour stem cells and drug resistance. Nat Rev Cancer 2005; 5: 275-284.

[4] Stewart DJ. Tumor and host factors that may limit efficacy of chemotherapy in non-small cell and small cell lung cancer. Crit Rev Oncol Hematol 2010; 75: 173-234.

[5] Robey RW, To KK, Polgar O, Dohse M, Fetsch P, Dean M and Bates SE. ABCG2: a perspective. Adv Drug Deliv Rev 2009; 61: 3-13.

[6] Zhou S, Schuetz JD, Bunting KD, Colapietro AM, Sampath J, Morris JJ, Lagutina I, Grosveld GC, Osawa M, Nakauchi H and Sorrentino BP. The ABC transporter Bcrp1/ABCG2 is expressed in a wide variety of stem cells and is a molecular determinant of the side-population phenotype. Nat Med 2001; 7: 1028-1034.

[7] Damiani D, Tiribelli M, Geromin A, Michelutti A, Cavallin M, Sperotto A and Fanin R. ABCG2 overexpression in patients with acute myeloid leukemia: Impact on stem cell transplantation outcome. Am J Hematol 2015; 90: 784-789.

[8] Kim YH, Ishii G, Goto K, Ota S, Kubota K, Murata Y, Mishima M, Saijo N, Nishiwaki Y and Ochiai A. Expression of breast cancer resistance protein is associated with a poor clinical outcome in patients with small-cell lung cancer. Lung Cancer 2009; 65: 105-111.

[9] Tsunoda S, Okumura T, Ito T, Kondo K, Ortiz C, Tanaka E, Watanabe G, Itami A, Sakai Y and Shimada Y. ABCG2 expression is an independent unfavorable prognostic factor in esophageal squamous cell carcinoma. Oncology 2006; 71: 251-258.

[10] Yoh K, Ishii G, Yokose T, Minegishi Y, Tsuta K, Goto K, Nishiwaki Y, Kodama T, Suga M and Ochiai A. Breast cancer resistance protein impacts clinical outcome in platinum-based chemotherapy for advanced non-small cell lung cancer. Clin Cancer Res 2004; 10: 1691-1697.

[11] Farajnia S, Ahmadzadeh V, Tanomand A, Veisi K, Khosroshahi S and Rahbarnia L. Development trends for generation of single-chain antibody fragments. Immunopharmacol Immunotoxicol 2014; 36: 297-308.

[12] Kazuma SM, Cavalcante MF, Telles AE, Maranhao AQ and Abdalla DS. Cloning and expression of an anti-LDL(-) single-chain variable fragment, and its inhibitory effect on experimental atherosclerosis. MAbs 2013; 5: 763-775.

[13] Deutscher S. Phage display in molecular imaging and diagnosis of cancer. Chem Rev 2010; 110: 3196-3211.

[14] Nelson A, Dhimolea E and Reichert J. Development trends for human monoclonal antibody therapeutics. Nat Rev Drug Discov 2010; 9: 767-774.
[15] Pande J, Szewczyk MM and Grover AK. Phage display: concept, innovations, applications and future. Biotechnol Adv 2010; 28: 849-858.
[16] Luo Y, Pang H, Li S, Cao H, Peng Z, Fan C and Li S. Production and radioimmunoimaging of novel fully human phage display recombinant antibodies and growth inhibition of lung adenocarcinoma cell line overexpressing Prx I. Cancer Biol Ther 2009; 8: 1369-1377.
[17] Williams GH and Stoeber K. The cell cycle and cancer. J Pathol 2012; 226: 352-364.
[18] Gottesman MM and Pastan IH. The Role of Multidrug Resistance Efflux Pumps in Cancer: Revisiting a JNCI Publication Exploring Expression of the MDR1 (P-glycoprotein) Gene. J Natl Cancer Inst 2015; 107.
[19] Roninson IB. The role of the MDR1 (P-glycoprotein) gene in multidrug resistance in vitro and in vivo. Biochem Pharmacol 1992; 43: 95-102.
[20] Wilson TR, Longley DB and Johnston PG. Chemoresistance in solid tumours. Ann Oncol 2006; 17 Suppl 10: x315-324.
[21] Zagryazhskaya A, Gyuraszova K and Zhivotovsky B. Cell death in cancer therapy of lung adenocarcinoma. Int J Dev Biol 2015; 59: 119-129.
[22] Jin Y, Bin ZQ, Qiang H, Liang C, Hua C, Jun D, Dong WA and Qing L. ABCG2 is related with the grade of glioma and resistance to mitoxantone, a chemotherapeutic drug for glioma. J Cancer Res Clin Oncol 2009; 135: 1369-1376.
[23] Steinbach D, Sell W, Voigt A, Hermann J, Zintl F and Sauerbrey A. BCRP gene expression is associated with a poor response to remission induction therapy in childhood acute myeloid leukemia. Leukemia 2002; 16: 1443-1447.
[24] Turner JG, Gump JL, Zhang C, Cook JM, Marchion D, Hazlehurst L, Munster P, Schell MJ, Dalton WS and Sullivan DM. ABCG2 expression, function, and promoter methylation in human multiple myeloma. Blood 2006; 108: 3881-3889.
[25] Larsen JE, Cascone T, Gerber DE, Heymach JV and Minna JD. Targeted therapies for lung cancer: clinical experience and novel agents. Cancer J 2011; 17: 512-527.
[26] Cagle PT and Chirieac LR. Advances in treatment of lung cancer with targeted therapy. Arch Pathol Lab Med 2012; 136: 504-509.
[27] Ritchie M, Tchistiakova L and Scott N. Implications of receptor-mediated endocytosis and intracellular trafficking dynamics in the development of antibody drug conjugates. MAbs 2013; 5: 13-21.
[28] Tortorella S and Karagiannis TC. Transferrin receptor-mediated endocytosis: a useful target for cancer therapy. J Membr Biol 2014; 247: 291-307.
[29] Ola MS, Nawaz M and Ahsan H. Role of Bcl-2 family proteins and caspases in the regulation of apoptosis. Mol Cell Biochem 2011; 351: 41-58.
[30] Rebillard A, Jouan-Lanhouet S, Jouan E, Legembre P, Pizon M, Sergent O, Gilot D, Tekpli X, Lagadic-Gossmann D and Dimanche-Boitrel MT. Cisplatin-induced apoptosis involves a Fas-ROCK-ezrin-dependent actin remodelling in human colon cancer cells. Eur J Cancer 2010; 46: 1445-1455.
[31] Stacy AE, Jansson PJ and Richardson DR. Molecular pharmacology of ABCG2 and its role in chemoresistance. Mol Pharmacol 2013; 84: 655-669.
[32] Mao Q and Unadkat JD. Role of the breast cancer resistance protein (BCRP/ABCG2) in drug transport--an update. AAPS J 2015; 17: 65-82.
[33] Dean M. ABC transporters, drug resistance, and cancer stem cells. J Mammary Gland Biol Neoplasia 2009; 14: 3-9.

Table S1. Primers for real-time PCR. Sequences of primers (5'-3') used for real-time PCR including the length of the PCR product and annealing temperature

Gene	Primer sequence (5'-3')	Product size (bp)	Annealing temperature (°C)
ABCG2 F	CACAAGGAAACACCAATGGCT		
ABCG2 R	ACAGCTCCTTCAGTAAATGCCTTC	69	55
GAPDH F	GAAGGTGAAGGTCGGAGTC		
GAPDH R	GAAGATGGTGATGGGATTTC	225	55

bp, base pair; F, Forward; R, Reverse.

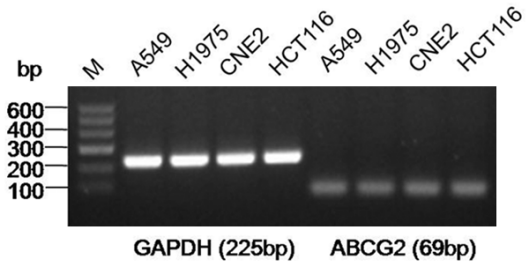

Figure S1. PCR and Western blot analyze the expression of the ABCG2 in different cell lines. The difference was not statistically significant.

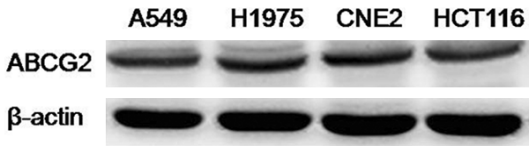

Figure S2. PCR and Western blot analyze the expression of the ABCG2 in different cell lines. The difference was not statistically significant.

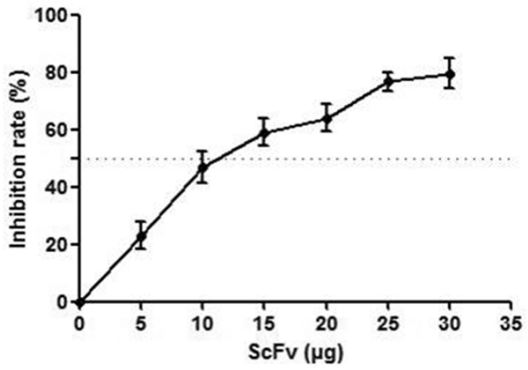

Figure S3. ScFv antibody concentration for achieving 50% growth inhibition of lung adenocarcinoma cells was determined by CCK-8 assay.

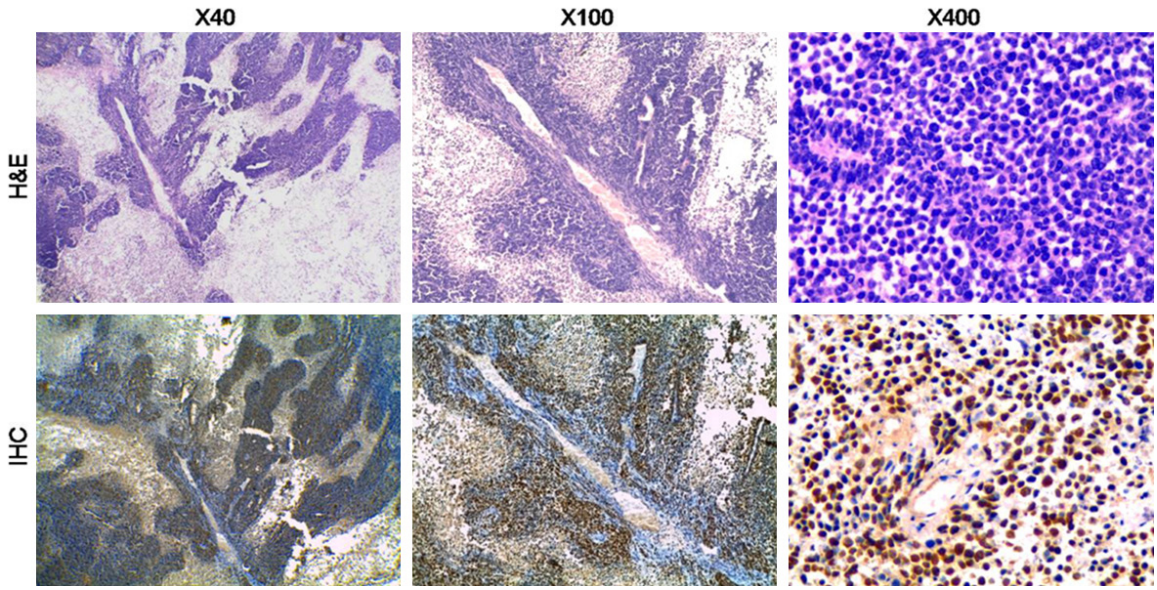

Figure S4. Haematoxylin and eosin (H&E) staining confirmed that the histological origin of the xenograft tumors were lung adenocarcinoma. Representative photomicrographs were provided (original magnification, × 40, × 100, × 400).